Conformational Flexibility of the Square-Pyramidal Coordination Cap in a Series of Octahedral Nickel(II) Pentaamine Complexes − Magnetochemical Characterization of the Singly μ-Cl-Bridged Nickel(II) Dimer [(pyN_4)Ni-Cl-Ni(pyN_4)](PF_6)$_3$ [pyN_4 = 2,6-Bis(1′,3′-diamino-2′-methylprop-2′-yl)pyridine]

Christian Dietz[a], Frank W. Heinemann[a][+], Jörg Kuhnigk[b][+], Carl Krüger[b][+], Michael Gerdan[c][++], Alfred X. Trautwein[c][++], and Andreas Grohmann*[a]

Institut für Anorganische Chemie, Universität Erlangen-Nürnberg,[a]
Egerlandstraße 1, D-91058 Erlangen, Germany
Fax: +49 (0)9131/857367
E-mail: grohmann@anorganik.chemie.uni-erlangen.de

Max-Planck-Institut für Kohlenforschung,[b]
Kaiser-Wilhelm-Platz 1, D-45470 Mülheim an der Ruhr, Germany

Institut für Physik, Medizinische Universität zu Lübeck,[c]
Ratzeburger Allee 160, D-23538 Lübeck, Germany

Received December 23, 1997

Keywords: Tetrapodal pentadentate ligand / Square pyramidal coordination cap / Pentaamine / Nickel(II) complexes / Magnetochemistry

The architecture of the tetrapodal pentaamine ligand 2,6-bis(1′,3′-diamino-2′-methylprop-2′-yl)pyridine (pyN_4, **1**) allows it to coordinate to nickel(II) as a square pyramidal coordination cap. The pyridine nitrogen atom occupies an apical position of the coordination octahedron, while four equivalent pendent primary amino groups occupy the equatorial positions, with a sixth coordination site remaining for a monodentate ligand. Exchange of this ligand is facile, and a series of complexes [(**1**)NiX]$^{n+}$ (X = OH_2, $OClO_3$, NCS, N_3, {Cl-Ni(pyN_4)}) has been prepared and characterised by elemental analysis, IR and UV/Vis spectroscopies (as applicable), and X-ray structure determination. While the solid state structures show varying degrees of distortion of the ligand cap **1** from C_{2v} symmetry, a polynucleating coordination mode has not been observed. The ligand enables the synthesis of dinuclear nickel(II) complexes containing a single bridging ligand, as exemplified by the singly μ-chloro bridged complex [(**1**)Ni–Cl–Ni(**1**)](PF_6)$_3$. This complex has an antiferromagnetically coupled ground state of total spin $S_T = 0$, as determined from variable-temperature magnetic susceptibility measurements.

Introduction

The objective of our work is to explore the potential of tetrapodal pentadentate ligands as mononucleating head groups in functional transition metal complexes. Ligands of this topology are virtually unknown. Specifically, we aim to create octahedral coordination compounds containing a square-pyramidal coordination cap (a pentadentate ligand) and a substrate (a monodentate ligand), which is bound at the sixth coordination site. Ideally, functional groups appended to the base of the coordination cap will provide an environment for the substrate in which it shows modulated reactivity. Such metal complexes would utilise the principles of simultaneous first- and second-sphere coordination[1][2].

In this context, we recently introduced a tetrapodal pentadentate ligand with an NN_4 donor set, consisting of a central pyridine and four equivalent primary amino nitrogen atoms (pyN_4, **1**)[3]. Structural characterization of a cobalt(III) chloro complex showed that the ligand provides the desired square pyramidal coordination cap. A square-pyramidally coordinating ligand of overall C_{2v} symmetry represents a novel structural motif in coordination chemistry since it has one central donor atom which occupies the apical position of a pyramid, while *four* equivalent pendent donor groups take the basal positions. In the case of octahedral complexes, such a coordination mode leaves a sixth site for the binding of a monodentate substrate. The tetrapodal pentadentate ligand **1** is particularly attractive in that it forces a sixth ligand to coordinate *trans* to a pyridine substituent. While this feature has been suggested to influence the overall reactivity with respect to ligand exchange in certain cases, experimental verification has so far been lacking[4]. A topological relative of **1** has recently been described[5], being virtually identical to a ligand previously used by Canty and co-workers in their studies of the coordination chemistry of palladium(II), where square-pyramidal coordination was not observed[6]. A different type of tetrapodal pentadentate ligand of C_2 symmetry involves a "superstructured"[7][8] porphyrin, *i. e.* the basal donor atoms are incorporated into a macrocyclic ring.[9]

As part of our studies directed toward the synthesis of functional metal complexes with a square-pyramidal coor-

[+] X-ray structure analyses. − [++] Magnetochemical measurements.

  1434−1948/98/0707−1041 $ 17.50+.50/0

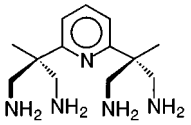

1

dination cap, we have been exploring the coordination behaviour of the pyN_4 ligand **1** and the reactivity of a variety of complex fragments of the type [(**1**)M] (M = Co, Ni, Rh), as well as the further derivatization of this ligand in order to construct a concave ligand periphery and/or an enclosed coordination site. We now wish to report our findings relating to ligand exchange at the fragment $[(\mathbf{1})Ni]^{2+}$, for which we have used the aqua complex $[(\mathbf{1})Ni(H_2O)]Cl_2$ (**2**) as precursor. We were interested in the structural characterization of the aqua complex as well as a series of other complexes $[(\mathbf{1})Ni(X)]^{n+}$ (X = perchlorate, halide, pseudohalide), in order to assess the influence, if any, of monodentate ligands X upon the coordination mode of the pentadentate ligand, and to obtain a quantitative measure of the flexibility of the ligand in those cases where it does provide a square-pyramidal coordination cap.

Exchange reactions have yielded the mono- and dinuclear nickel(II) complexes $[(\mathbf{1})Ni(H_2O)]I_2$ (**4**), $[(\mathbf{1})Ni(OClO_3)](ClO_4)$ (**5**), $[(\mathbf{1})Ni(\mu\text{-}Cl)Ni(\mathbf{1})](PF_6)_3$ (**6**), $[(\mathbf{1})Ni(NCS)](PF_6)$ (**7**), and $[(\mathbf{1})Ni(N_3)](PF_6)$ (**8**). While the solid state structures of these compounds show different degrees of distortion of the ligand cap, the pentaamine ligand **1** does act as a podand in all cases, and a polynucleating coordination mode (which is undesirable in the light of the aims specified above) is not observed. Since the pentadentate ligand effectively blocks five coordination sites in a coordination octahedron, it allows the synthesis of dinuclear complexes containing a single bridging ligand. In view of the interest attached to such complexes, particularly with respect to their magnetic properties[10], we have undertaken the magnetochemical characterization of the dinuclear μ-chloro-bridged nickel(II) complex **6**.

Results and Discussion

Analytical data indicate the nickel(II) aqua complex $[(\mathbf{1})Ni(H_2O)]Cl_2$ (**2**) to be the primary species formed when an ammoniacal aqueous solution of the tetrakis(hydrochloride) salt **1** • 4 HCl (ref.[3]) is treated with one equivalent of $NiCl_2 \bullet 6\ H_2O$. Drying of the purple crystalline material in vacuo results in a colour change to bluish green which indicates removal of the aqua ligand. Addition of $NaClO_4$ to an aqueous solution of **2** and recrystallization of the resulting precipitate from water/methanol (1:1 v/v) gives a crystalline solid (**3**) with no conclusive elemental analysis and IR data. Preliminary X-ray structural data of this solid confirm the pyN_4 ligand to act as a square-pyramidal coordination cap and reveal the presence of at least one uncoordinated perchlorate anion, but do not allow the identification of the monodentate ligand at the sixth coordination site. The residual electron density is compatible with a ligand containing a single "heavy" atom, and both chloride and water are likely candidates, but neither enables further refinement. Hence, the possibility of this substance being a mixture of the chloro and aqua complexes cannot be ruled out.

$[(\mathbf{1})Ni(H_2O)]I_2$ (4)

Exchange of the monodentate ligand is facile in **2** and **3**, and the above results suggest chloride and water compete as ligands for the sixth coordination site. The aqua complex is formed exclusively as the iodide salt $[(\mathbf{1})Ni(H_2O)]I_2$ (**4**) upon recrystallization of **2** from water in the presence of an excess of sodium iodide. These conditions apparently prevent the coordination of chloride, while the large iodide ligand, if accommodated, would induce steric strain as a consequence of van der Waals interactions with the basal amino groups of the complex fragment $[(\mathbf{1})Ni]^{2+}$ (ref.[11]).

The spectroscopic characteristics of **4** resemble those determined for the other complexes in the present series (**5**, **6**, **7**, and **8**). All complexes contain octahedrally coordinated high-spin nickel(II), making ^1H NMR spectra of limited diagnostic value due to paramagnetically shifted and broadened resonances (an assignment is given below for the proton spectrum of **5**, based on approximate integration intensities and chemical shifts). The UV/Vis spectrum of an aqueous solution of **4** is characterized by an absorption attributable to a d-d transition at $\lambda = 543$ nm ($\varepsilon = 3.4\ dm^3\ mol^{-1}\ cm^{-1}$), in keeping with data obtained for other six-coordinate polyamine complexes of Ni(II)[12]. The spectrum is virtually identical to those of complexes **5**, **6**, **7**, and **8**, presumably due to the ease of ligand exchange at the sixth coordination site.

The IR spectrum of **4** shows bands characteristic of N−H, O−H, and skeletal vibrations of the ligand [in particular, the ν(C=C) and ν(C=N) in-plane vibrations of the pyridine ring]. The base peak in the FD mass spectrum is at $m/z = 436$ ($[(\mathbf{1})NiI]^+$), all other peaks having an intensity of less than 10%. In the FAB spectrum, the base peak is again at $m/z = 436$, with a fragment ion at $m/z = 309$ ($[(\mathbf{1})Ni]^+$, 45%). These results indicate that exchange of the aqua ligand for an iodo ligand does occur under the conditions prevailing in the mass spectrometer.

Compound **4** crystallises in the monoclinic space group $P2_1/n$. The molecular structure of the cation, which has no crystallographically imposed symmetry, is shown in Figure 1. The nickel(II) ion is coordinated by the pentaamine ligand **1** in pyramidal fashion, leading to the formation of six six-membered chelate rings, all of which adopt a boat conformation. The aqua ligand completes the Ni(II) coordination octahedron. It forms two weak hydrogen bonds to the two iodide counterions [d(O1···I1) = 3.406(4) A, d(O1···I2) = 3.405(3) A; sum of the van der Waals radii of O and I: 3.50 A[13]]. The arrangement of the equatorial nitrogen atoms around the nickel centre is trapezoidal rather than square planar, with two shorter and two longer $Ni-N_{eq}$ bond distances (Table 1). The angles $N_{eq}-Ni-N_{eq}$ in the NiN_4 plane have average values of 84.9(2)° and 95.2(2)° for diametrically opposite pairs, the smaller value representing the averaged "bite angle" of the 1,3-diaminoprop-2-yl substituents. These groups are displaced slightly

toward the equatorial NiN_4 unit, as indicated by the deviations of the angles at the *ortho* carbon atoms from their ideal values of 120° [N11−C11−C18 116.8(3)°; C12−C11−C18 122.7(4)°; N11−C15−C22 116.7(3)°; C14−C15−C22 122.8(4)°]. Whether this is a consequence of the ligand acting as a podand toward the central nickel ion cannot be said with certainty as similar deviations are observed for the corresponding angles in the tetrakis(hydrobromide) salt **1** • 4 HBr where the *ortho* substituents are not constrained by metal coordination[14]. However, the Ni−N_{ax} bond length at 2.050(3) A is shorter than the average Ni−N_{eq} bond length [2.090(4) A]. By way of comparison, the corresponding Ni−N_{py} bond lengths in the cation $[(H_2O)_5Ni(py)]^{2+}$ and in a Ni(II) cyclam complex with a pendent pyridyl group coordinated *trans* to an aqua ligand are 2.08(1) A[15] and 2.142(4) A[16], respectively, while the averaged Ni−N_{eq} bond length in the latter complex is 1.927(5) A. The nickel−oxygen bond length in **4** [d(Ni−O) = 2.133(3) A] is within the range of values found in both the pentaaqua and the cyclam complexes [*d*(Ni−O) = 2.05(1)···2.18(1) A[15], and *d*(Ni−O) = 2.166(3) A[16], respectively].

Figure 1. Molecular structure of the cation in **4** with thermal ellipsoids drawn at the 50% probability level; hydrogen atoms are omitted for clarity

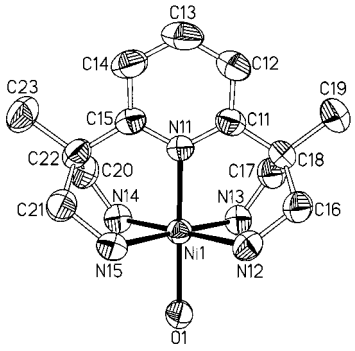

As shown in the side-on view in Figure 2, the $[(pyN_4)Ni]^{2+}$ complex fragment in **4** is distorted from C_{2v} symmetry. The pyridine ring, itself a regular hexagon, is tilted to one side of the (pyN_4)Ni pyramid, inducing a slight bending of the N_{ax}−Ni−O axis relative to the equatorial NiN_4 unit (cf. Table 1 for relevant bond angles N_{ax}−Ni−N_{eq}). This unit shows minor tetrahedral distortion, with diagonally opposite N donor atoms 0.015(4) A above and, respectively, below the plane containing the nickel atom. For the purpose of comparison with the other structures reported in the present publication, the distortion of the ligand cap in **4** from C_{2v} symmetry may be quantified as follows (Table 2): a) The least-squares planes defined by the pyridine ring (N11, C11, C12, C13, C14, C15) on the one hand and the quaternary and methyl carbon atoms C18, C19, C22, C23 on the other do not coincide but form a dihedral angle of 15.4(4)°; b) the least-squares planes defined by the four methylene carbon atoms C16, C17, C20, C21 and the four equatorial amino nitrogen atoms N12, N13, N14, N15 are not parallel but at a dihedral angle of 8.0(1)°; c) one of the distances between pairs of equivalent methylene carbon atoms in the two 1,3-diaminoprop-2-yl groups [*d*(C16···C21)] is widened to a value of 5.399(7) A, while the other [*d*(C17···C20)] is compressed to 4.743(7) A. This distortion (see below for a unifying discussion of possible causes) attests to the flexibility of the ligand backbone. Except for the angles given in Table 1, all other angles in the carbon framework are close to the ideal values expected for sp^2 and sp^3 carbon and nitrogen atoms, respectively.

[(1)Ni(OClO$_3$)](ClO$_4$) (5)

Recrystallization of the ill-defined complex **3** from methanol in the presence of $NaClO_4$ yields single crystalline material whose IR spectrum is characterised by a triply split very intense band between 1088 and 1145 cm^{-1} (ClO_4 str). This is characteristic of unidentate perchlorate coordination (reduction of the local symmetry from T_d to C_{3v})[17] and points to the perchlorato perchlorate complex [(**1**)Ni(OClO$_3$)](ClO$_4$) (**5**). Its ^{1}H NMR spectrum ([D$_6$]DMSO, room temp.) shows paramagnetically shifted resonances over the range 0 to + 140 ppm which can be assigned on the basis of their approximate integration intensities and are in accord with C_{2v} symmetry of the pyN_4 ligand in the complex[18]. As expected, the protons closest to the nickel atom ($-NH_2$, $-CH_2-$) show the most pronounced paramagnetic shifts (128 and 100 ppm, respectively) and the largest line widths. The H^3 (*meta*), H^4 (*para*) and $-CH_3$ protons have signals at 43, 20, and 1 ppm, respectively, with line widths decreasing in this order, which mirrors the increasing remoteness of the proton locations with respect to the nickel center.

The X-ray structural study of **5** shows the cation to have C_1 symmetry in the solid state (Figure 2). The nickel atom is coordinated in distorted octahedral fashion by the pentadentate pyN_4 ligand and an oxygen atom of one of the perchlorate anions. While the diametrically related sets of bond angles N_{eq}−Ni−N_{eq} are comparable to the corresponding values in **4**, the N_{py}−Ni−O unit deviates significantly from linearity [N11−Ni1−O1 166.0(5)°]. However, the coordination cap in **5** is less distorted than in **4**, as is evident from the structural parameters listed in Table 2, which are closer to the ideal values. The Ni−N_{ax} bond is shorter still in **5** [Ni1−N11 2.015(4) A] than in **4** [2.050(3) A], while the average Ni−N_{eq} bond lengths are comparable [**5**: 2.09(1) A; **4**: 2.090(4) A]. The bond length in **5** between nickel and the oxygen atom of the coordinated perchlorate anion has a value of *d*(Ni1−O1) = 2.233(6) A which is shorter than the value found in the nickel(II) perchlorato complex of a pendant-arm macrocyclic ligand which also has an N_5 donor set [*d*(Ni−O) = 2.393(8) A][19]. The bond lengths and angles within both perchlorate anions are in the normal range.

[(1)Ni(μ-Cl)Ni(1)](PF$_6$)$_3$ (6)

Recrystallization of **2** from water in the presence of NH_4PF_6 gives a purple material, and analytical data suggest it is the bridged species [(**1**)Ni(μ-Cl)Ni(**1**)](PF$_6$)$_3$ (**6**). Its formation requires partial dissociation of the monodentate ligand in **2**, in accord with the observation that a vacant coordination site may be created in a complex by NH_4PF_6-induced loss of a labile ligand[20]. Compound **6**, once

Table 1. Selected bond lengths [Å] and angles [°] for **4**, **5**, **6**, **7** and **8** with estimated standard deviations in parentheses

bond or angle	**4**	**5**	**6**	**7**	**8**
Ni1−N11	2.050(3)	2.015(4)	2.05(1)	2.062(4)	2.062(5)
Ni1−N12	2.108(3)	2.01(1)	2.09(1)	2.113(5)	2.119(6)
Ni1−N13	2.068(4)	2.16(1)	2.08(1)	2.110(5)	2.080(6)
Ni1−N14	2.073(4)	2.10(1)	2.07(1)	2.098(6)	2.054(6)
Ni1−N15	2.110(4)	2.08(1)	2.10(1)	2.132(6)	2.106(5)
Ni1−X[a]	2.133(3)	2.233(6)	2.448(2)	2.086(4)	2.156(5)
N11−Ni1−N12	87.2(1)	90.8(4)	89.4(5)	88.8(2)	85.5(2)
N11−Ni1−N15	88.2(1)	91.1(5)	87.5(5)	88.8(2)	85.5(2)
N11−Ni1−N13	92.9(1)	89.0(4)	90.5(5)	90.9(2)	91.3(2)
N11−Ni1−N14	92.3(1)	90.9(4)	90.9(5)	89.8(2)	90.9(2)
N12−Ni1−N13	85.2(2)	88.5(3)	85.8(5)	83.9(2)	85.9(3)
N14−Ni1−N15	84.6(2)	84.7(2)	85.2(5)	84.2(3)	86.6(3)
N13−Ni1−N14	96.3(2)	91.5(5)	94.9(5)	96.6(2)	95.1(3)
N12−Ni1−N15	94.0(2)	95.3(6)	94.1(6)	95.3(3)	92.2(3)
N12−Ni1−N14	178.5(2)	178.3(5)	179.2(5)	178.5(2)	176.3(2)
N13−Ni1−N15	178.6(2)	176.2(5)	177.9(5)	179.1(2)	176.4(3)
N11−Ni1−X[a]	179.32(13)	166.0(5)	178.4(3)	177.1(2)	175.1(2)
Ni1−N12−C16	115.7(3)	118.3(9)	117(1)	116.9(4)	115.9(4)
Ni1−N13−C17	113.6(3)	113.8(8)	116(1)	117.0(3)	114.0(4)
Ni1−N14−C20	114.0(3)	114.8(7)	116(1)	117.0(4)	114.1(4)
Ni1−N15−C21	116.0(3)	116.8(9)	115(1)	115.9(4)	116.0(4)
N12−C16−C18	114.2(4)	115(1)	115(1)	115.4(5)	113.2(5)
N13−C17−C18	113.9(4)	116(1)	113(1)	113.8(5)	115.1(6)
N14−C20−C22	114.5(4)	120(1)	113(1)	114.8(5)	114.5(5)
N15−C21−C22	114.0(3)	112(1)	118(1)	117.3(5)	112.7(5)

[a] **4**: X = O1; **5**: X = O1; **6**: X = Cl1; **7**: X = N1; **8**: X = N21.

formed and isolated, may be recrystallised from water. Whether or not the dinuclear species persists in aqueous solution is uncertain as the UV-Vis spectrum is not significantly different from that of the mononuclear aqua complex **4**. The X-ray structural analysis of **6** confirms the presence of a dinuclear chloro-bridged complex cation in the solid state, making it one of the very few structurally characterised complexes containing a single *unsupported* Ni(II)−X−Ni(II) halide bridge[21]. The compound crystallises in the tetragonal space group $I4_1cd$, and the two halves of the molecule are related by a two-fold rotation axis which bisects the Ni−Cl−Ni′ unit (Figure 3). The bridging chloro substituent (Cl1) and the phosphorus atom of one of the three PF_6^- counterions occupy special positions. The coordination mode of the pentaamine ligand **1** is again pyramidal. The chloro substituent functions as a bridge between two symmetry-equivalent nickel(II) ions, the angle subtended at the μ-chloro ligand by the bonds to Ni1 and Ni1′ being 165.5(3)°. Similar to **4** and **5**, the angles $N_{eq}-Ni-N_{eq}$ in the NiN_4 plane have average values of 85.5(5)° and 94.5(6)° for diametrically opposite pairs, leading to a rectangular rather than a square arrangement of the equatorial amino nitrogen atoms around the nickel centre (Table 1). The C_2 symmetry of the dinuclear ion causes the equatorial NiN_4 unit and its symmetry-related counterpart to adopt an eclipsed conformation. The $Ni-N_{ax}$ bond length (2.049(11) Å) is again shorter than the average $Ni-N_{eq}$ value [2.085(13) pm], but the higher standard deviations in this structure limit the usefulness of this comparison. The Ni−Cl bond length of 2.448(2) Å is appreciably shorter than in two other complexes containing octahedrally coordinated nickel(II) bridged by a single μ-chloro ligand [*d*(Ni−Cl) = 2.941(2) Å[22] and 2.712(4) Å (average)[23], respectively]. The capping pentaamine ligand is again distorted in the sense that the pyridine ring is tilted to one side of the $[NN_4]$Ni pyramid, the degree of distortion being comparable to that observed in **4** (cf. Table 2 for relevant distances and interplanar angles). The hexafluorophosphate counterions show thermal disorder but otherwise have normal structural parameters.

[(1)Ni(NCS)](PF$_6$) (7)

In view of the ready formation of a dinuclear complex from **2** by incorporation of a μ-chloro ligand under suitable conditions, we carried out substitution experiments with potentially bidentate polyatomic anions such as thiocyanate or azide in the anticipation of obtaining dinuclear species containing end-to-end coordinated, μ-(1,3)-pseudohalide bridges. Such complexes are of current interest with respect to their magnetic properties[24][25][26]. So far, however, even in the presence of NH_4PF_6, these reactions have yielded only the mononuclear complexes[27], which X-ray structural analyses have shown to contain terminally coordinated pseudohalide ligands.

The IR spectrum of the complex [(**1**)Ni(NCS)](PF_6) (**7**) is inconclusive with respect to the bonding mode of the SCN^- ligand. The X-ray crystal structure determination shows **7** to be the isothiocyanato complex, its cation having the expected octahedral symmetry. The distortion of the pyN_4 ligand in **7** (Figure 2) is much less severe than in complexes **4** and **6**, and comparable to that in **5**. The least-squares planes defined by the four methylene carbon atoms C16, C17, C20, C21 and the four equatorial amino nitrogen atoms N12, N13, N14, N15 form an angle of only 3.0(2)°, and the distances between pairs of equivalent methylene carbon atoms in the two 1,3-diaminoprop-2-yl groups

Figure 2. Molecular structures of the cations in **4** (top left), **5** (top right), **7** (bottom left), and **8** (bottom right); side-on views are shown in order to illustrate the differing degrees of distortion of the ligand caps; for clarity, ball-and-stick representations have been chosen, and all hydrogen atoms have been omitted; for all structures, the numbering of atoms in the pyridine ring is identical to that shown in Figure 1

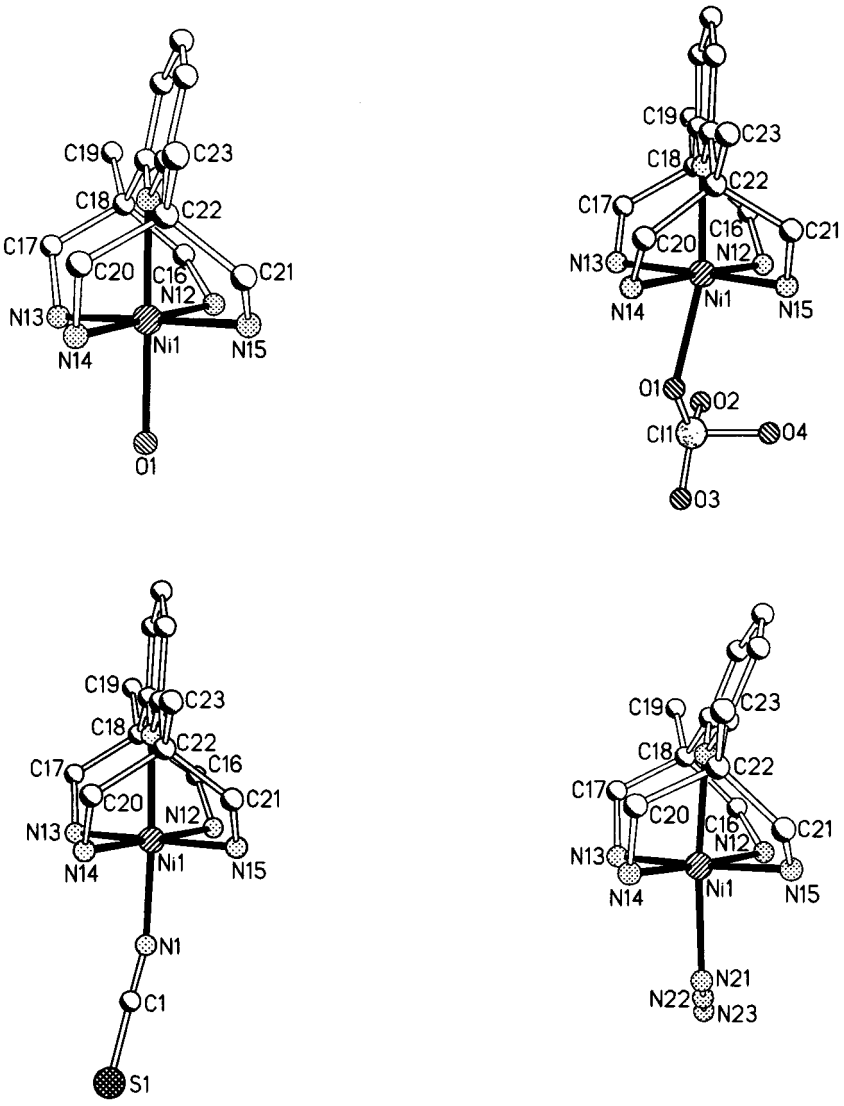

Table 2. Intramolecular angles [°] and distances [Å] illustrating the distortion of the ligand cap in complexes **4**, **5**, **6**, **7** and **8** (with estimated standard deviations in parentheses); see footnote and text for definitions of angles

bond or angle	**4**	**5**	**6**	**7**	**8**
ε[a]	15.4(4)	1(1)	17(1)	5.0(3)	26.8(4)
ζ[b]	8.0(1)	1.3(3)	7.4(4)	3.0(2)	9.8(2)
η[c]	11.6(2)	3.1(6)	13.2(6)	4.0(2)	19.3(2)
d(C16···C21)	5.399(7)	5.18(2)	5.30(3)	5.28(1)	5.44(1)
d(C17···C20)	4.743(7)	5.01(2)	4.80(3)	5.06(1)	4.69(1)

[a] Angle ε between the least-squares planes defined by the pyridine ring (N11, C11, C12, C13, C14, C15) and the quaternary and methyl carbon atoms C18/C19/C22/C23. – [b] Angle ζ between the least-squares planes defined by the equatorial nitrogen atoms N12/N13/N14/N15 and the methylene carbon atoms C16/C17/C20/C21. – [c] Angle η subtended by the lines N11···C13 and N11–Ni1 at N11.

[*d*(C16···C21) and d(C17···C20)] have adjusted to 5.28(1) Å and 5.06(1) Å, respectively. On average, the Ni–N_{eq} bonds in **7** are slightly longer and the Ni–N_{eq}–C angles slightly larger than in the other complexes, and it appears that these differences, and possibly also solid state packing effects, allow the ligand to adopt a conformation closer to C_{2v} symmetry. The isothiocyanato ligand is linear [N1–C1–S1 = 177.8(6)°] and is coordinated to nickel at an angle of

Figure 3. Molecular structure of the cation in **6**; hydrogen atoms have been omitted for clarity; the numbering of atoms in the pyridine ring is identical to that shown in Figure 1

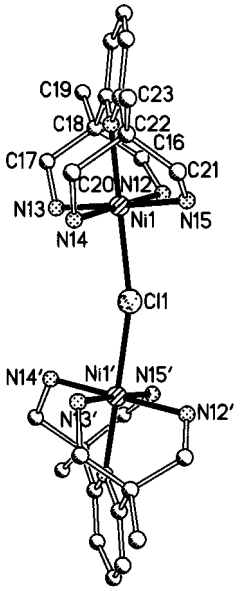

Ni1−N1−C1 = 165.9(5)°, with an Ni1−N1 bond length of 2.086(4) A. Corresponding values for an octahedral nickel(II) complex likewise containing a *trans* py−Ni−NCS unit are 159.0(3)° and 2.022(3) A, respectively[28].

[(1)Ni(N$_3$)](PF$_6$) (8)

The IR spectrum of the azide complex [(**1**)Ni(N$_3$)](PF$_6$) (**8**) shows, in addition to diagnostic bands due to the pyN$_4$ ligand and the hexafluorophosphate counterion, a sharp and very intense band at 2060 cm^{-1} due to the asymmetric stretching vibration of the coordinated azide ligand. Structural analysis reveals a complex cation (Figure 2) in which the distortion of the ligand cap is the most pronounced of all the complexes in the present series. While the Ni−N$_{py}$ bond length *trans* to the azide ligand [*d*(Ni1−N11) = 2.062(5) A] is identical to the corresponding value found in the isothiocyanate complex **7** (Table 1), the pyridine ring (which is planar to within 4 σ) is forced out of coplanarity with the quaternary and the exocyclic methyl carbon atoms of the ligand backbone by 26.8(4)° (Table 2). More significantly than in the other structures, the Ni−N$_{py}$ bond Ni1−N11 is bent from its vertical orientation relative to the NiN$_4$ plane, with relevant angles N$_{ax}$−Ni−N$_{eq}$ ranging from 85.5(2)° to 91.3(2)°. Further distances and angles are given in Table 1, and the complete set of parameters quantifying the ligand distortion in comparison to the other structures is given in Table 2. It is interesting to note that, despite the more serious distortion of the ligand in **8** with respect to the relative orientation of the pyridine ring, the bond angles in the carbon backbone (especially those at the methylene carbon atoms of the 1,3-diaminoprop-2-yl units, cf. Table 1) do not differ significantly from the corresponding values in the other structures. The terminally-coordinated azide ligand is linear [N21−N22−N23 = 177.9(7)°], and is bound to the nickel centre at an angle of Ni1−N21−N22 = 116.4(4)° (an angle approaching 120° is to be expected[29]; corresponding angles in other octahedral Ni(II) complexes containing terminal azide ligands span the range 123···138°[27][30][31][32][33][34]). The bond length *d*(Ni−N$_\alpha$) at 2.156(5) A is somewhat longer than in other terminal nickel(II) azide complexes (2.05···2.12 A)[27][30][31][32][33][34].

The Conformation of the Ligand Cap in 4, 5, 6, 7, and 8

The factors responsible for the varying degrees of distortion of the pentaamine ligand **1** in the solid state structures of **4**, **5**, **6**, **7**, and **8** are difficult to assess. The ligand has the topology of a podand, and hence is inherently more flexible than a macrocyclic or a cage-like arrangement of donor atoms, with their higher degrees of preorganization ("juxtapositional fixedness"[7]). The structures of complexes of **1** in the solid state are therefore expected to be more susceptible to packing effects, the significance of which will vary depending on the nature of the monodentate ligand and of the counterions. On a more subtle level, the *trans* influences ("static *trans* effects"[35][36]) of the monodentate ligands have to be considered. Perchlorate is weakly bound, and its complex has a shorter Ni−N$_{py}$ bond than the other complexes in the series. The tilt of the pyridine ring, however, is obviously unrelated to the length of the bond connecting it to the metal centre (i. e., the *trans* effect of the monodentate ligand). Thus, the isothiocyanato complex **7** and the azide complex **8**, while differing markedly in the degree of distortion of the ligand cap, have Ni−N$_{py}$ bond lengths which are identical within experimental error.

Magnetic Properties of 6

The magnetic behaviour of di- and polynuclear transition metal complexes is being studied extensively. The objective is to define the role played by the bridging ligands in mediating coupling interactions between the paramagnetic metal centers, and in particular to establish magneto-structural correlations[10]. Nickel(II) complexes, especially those containing chain-like one-dimensional arrangements of alternating metal atoms and bridging ligands, feature prominently in this context[29][32][37][38][39]. Bridging groups include carboxylato, nitrito, cyanide, cyanato, thiocyanato and, in particular, azido ligands, and complexes containing single, double, and triple bridges have been characterised[38][39][40]. The scarcity of polynuclear nickel(II) compounds containing an unsupported single halide bridge[21] led us to undertake the magnetochemical characterization of the μ-chloro bridged complex **6**.

The solid-state magnetic susceptibility of **6** was measured at 1.0 T in the temperature range 2 to 295 K using a SQUID magnetometer (MPMS, Quantum Design). Figure 4 shows the variation of both the molar paramagnetic susceptibility χ_M and the effective magnetic moment μ_{eff} (per mol) with temperature. As temperature decreases, χ_M increases slightly, reaching a broad maximum at 225 K, and then decreases to reach a minimum at 30 K. The marked rise of χ_M for T < 20 K is attributed to the presence of a small amount of paramagnetic impurity, presumed to be a monomeric nickel com-

plex. As may be seen from the plot of μ_{eff} versus T, the value of the effective magnetic moment decreases steadily with decreasing temperature from the maximum value of 3.17 μ_B at 295 K ($\chi_M \cdot T = 1.256$ cm^3 K mol^{-1}), reaching a minimum of 0.32 μ_B ($\chi_M \cdot T = 0.013$ cm^3 K mol^{-1}) at temperatures below 25 K. The theoretical spin-only value of the magnetic moment μ_{SO} for two uncoupled Ni(II) spins $S_{Ni} = 1$ is 4 μ_B ($\chi_M \cdot T = 2$ cm^3 K mol^{-1}), which is higher than the experimental value of 3.17 μ_B at 295 K. The data are, however, consistent with strong antiferromagnetic exchange between the two nickel atoms through the bridging chlorine atom, resulting in a diamagnetic ground state with total spin $S_T = 0$. The residual value of μ_{eff} is indicative of the presence of a paramagnetic impurity. The experimental data of **6** have been analysed by a least-squares fit procedure using an isotropic Heisenberg-Dirac-van-Vleck (HDVV) exchange Hamiltonian $H = -2J\,\boldsymbol{S}_1 \cdot \boldsymbol{S}_2$, and taking account of Zeeman splitting as well as corrections for paramagnetic impurity (p) and temperature-independent paramagnetism (TIP)[41]. Diamagnetic correction is based on substracting the sample-holder signal and the contribution $\chi_D = -236 \times 10^{-6}$ cm^3 mol^{-1}, as determined from Pascal's constants[10], from the raw data. A good fit was achieved (solid lines in Figure 4) for isotropic exchange coupling $J = -74$ cm^{-1} between the two paramagnetic sites, average g value $g = 2.18$, paramagnetic impurity with spin $S = 1$ and relative amount $p = 2.7\%$, and TIP = $+171\times10^{-6}$ cm^3 mol^{-1} per nickel atom. It was further assumed that the paramagnetic impurity has about half the molecular weight and half the diamagnetic correction χ_D of **6**. The J value for **6** is considerably larger than the values typically found for antiferromagnetic coupling in Ni(II) chains containing single μ-(1,3)-azido bridges[29,38,42,43] or multiple bridges[44][45][46][47][48][49]. The reason for **6** having such a large J value is that its Ni(II)−X−Ni(II) angle comes closest to 180° of all the Ni(II) chains considered. The g value is as expected for octahedral nickel(II) complexes (cf. the typical value of $g = 2.25$ for $[Ni(H_2O)_6]^{2+}$ [50]). As far as we are aware, **6** is the first complex containing a single halogen bridge between two Ni(II) centres that has been characterised by a magnetochemical method.

Summary

The tetrapodal pentaamine ligand **1** acts as a square-pyramidal coordination cap towards nickel(II) ions in aqueous solution, leaving a sixth site for the binding of a monodentate ligand, which completes the coordination octahedron. Exchange of the monodentate ligand is facile, and the pentadentate ligand shows considerable conformational flexibility, as illustrated by the solid state structures of the aqua, perchlorato, isothiocyanato, and azido complexes. Since the pentaamine ligand effectively blocks five coordination sites in a coordination octahedron, dinuclear Ni(II) complexes containing a single bridging ligand may also be prepared. The ligand thus meets the requirements set out in the Introduction for the construction of coordination caps carrying a functional periphery. Work using the complex fragment $[(\mathbf{1})Ni]^{2+}$ as a template for the derivatization of the tetrapodal pentadentate ligand **1** is currently in progress.

Figure 4. Temperature dependence of the effective magnetic moment μ_{eff} (Bohr magnetons, μ_B) and of the molar magnetic susceptibility χ_M (10^{-3} cm^3 mol^{-1}) of **6**. Squares and dots represent the experimental data, whereas the solid lines are the calculated fits (see text). The scales at left and right have been chosen so as to avoid overlay of the curves.

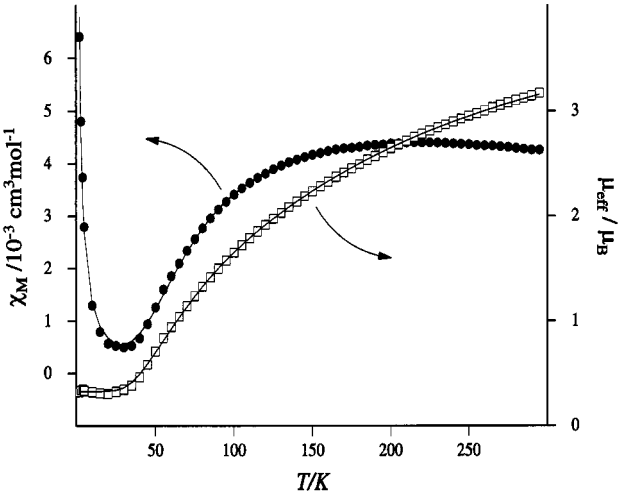

We thank Professor *D. Sellmann* for generous support of this work and Dr. *F. Hampel* for establishing the crystallographic data set of compound **8**. Further, a Liebig-Stipendium from the *Fonds der Chemischen Industrie* (to A. G.) is gratefully acknowledged.

Experimental Section

CAUTION! Although no problems were encountered in this work, transition metal perchlorate and azide complexes with organic ligands are potentially explosive and should be handled with due precautions.

Materials and Instrumentation: 2,6-$C_5H_3N\{CMe(CH_2NH_2)_2\}_2$ (**1**) was prepared as described previously[3]. The aqua complex **2** was prepared by reacting equimolar amounts of **1** • 4 HCl and $NiCl_2$ • 6 H_2O in dilute aqueous ammonia solution and subsequent cation exchange chromatography on Sephadex SPC-25. The chromatography was performed as described in a published procedure[51]. Reagents were AR grade or better and were purchased from Merck, Fluka, and Aldrich. IR (KBr discs) and UV/Vis spectra (solvent: water) were recorded on Perkin-Elmer 16PC FT-IR and Shimadzu UV-3101 PC instruments, respectively. NMR spectra were measured on a JEOL JNM-EX 270 spectrometer, and mass spectra were obtained on a JEOL MSTATION 700 spectrometer. Elemental analyses were performed using a Carlo Erba Elemental Analyzer 1106. Magnetic measurements were carried out on a polycrystalline sample with a SQUID magnetometer (MPMS, Quantum Design).

X-ray Crystallography: Crystal data for compounds **4**, **5**, **6**, **7**, and **8** are given in Table 3, and selected distances and angles are listed in Table 1. The structures of the cations are presented in Figures 1, 2, and 3. Only the cation of **5** shows slight disorder (oxygen atoms of the perchlorato ligand). The structure of **4** was solved by direct methods and refined using the programme package SHELXTL 5.03[52]. An absorption correction (Ψ scans, 10 reflections, $T_{min} = 0.011$, $T_{max} = 0.032$) was carried out. All non-hydrogen atoms were refined anisotropically (full-matrix least-squares). All hydrogen atoms were located in a difference Fourier synthesis, and all hydrogen atoms except H1A and H1B (aqua ligand) were refined isotropically. Both the positional and the isotropic displace-

ment parameters of H1A and H1B were kept constant during refinement. The structure of **5** was solved by direct methods (SHELXS-86) and refined on F^2 using SHELXL 93[53][54]. The structure of **6** was solved by direct methods and refined using the programme package SHELXTL 5.03. For both **5** and **6**, the non-hydrogen atoms were refined anisotropically (full-matrix least-squares), and the hydrogen atoms were positioned geometrically. The structures of **7** and **8** were solved by direct methods and refined using the programme package SHELXTL 5.03. For both structures, all non-hydrogen atoms were refined anisotropically (full-matrix least-squares), and all hydrogen atoms were located in a difference Fourier synthesis and refined isotropically. Crystallographic data (excluding structure factors) for the structures reported in this paper have been deposited with the Cambridge Crystallographic Data Centre as supplementary publication no. CCDC-100 937. Copies of the data can be obtained free of charge on application to CCDC, 12 Union Road, Cambridge CB2 1EZ, UK [Fax: int. code +44 (1223) 336−033; E-mail: deposit@ccdc.cam.ac.uk].

*[(**1**)Ni(H$_2$O)]I$_2$* (**4**): To a solution of **2** (0.94 g, 2.36 mmol) in water (50 ml) was added solid NaI (3.70 g, 24.69 mmol), and the mixture was stirred until all solid had dissolved. The solution was taken to dryness, the remaining solid taken up in as little methanol as possible, and the suspension filtered to remove NaI. Slow evaporation of solvent from the purple filtrate yielded a purple crystalline solid after several days. This was removed by filtration and air-dried. Yield: 0.40 g (0.69 mmol, 29%). Recrystallization from methanol gave single crystals suitable for an X-ray structure analysis. − IR (KBr): ν = 3272 cm^{-1} (br, OH/NH str), 2930 (CH str), 1594 (OH/NH def and C=C/C=N str), 1577 (OH/NH def and C=C/C=N str), 1463 (CH_2 asym def), 1397 (CH_2 sym def), 1024 (C−C skelet), 838 (NH def and CH_{pyr} oop def), 573 (C−C def). − UV/Vis (water): λ_{max} (ε) = 543 nm (3.4 dm^3 mol^{-1} cm^{-1}), 262 (1643). − MS (FD); *m/z* (%): 436 (100) [[(**1**)NiI]$^+$]; (FAB); *m/z* (%): 436 (100) [[(**1**)NiI]$^+$], 309 (45) [[(**1**)Ni]$^+$]. − $C_{13}H_{27}I_2N_5NiO$ (581.91): calcd. C 26.83, H 4.68, N 12.04; found C 26.66, H 4.26, N 11.98.

*[(**1**)Ni(OClO$_3$)](ClO$_4$)* (**5**): To a solution of **2** (0.42 g, 1.00 mmol) in water (5 ml) was added a saturated aqueous solution of $NaClO_4$ (5 ml). The resulting purple precipitate was centrifuged, washed with cold water, and dried in vacuo. Recrystallization from water/methanol (1:1 v/v) gave a crystalline solid (**3**) with no conclusive elemental analysis and IR data. A methanol solution of **3** (5 ml) containing $NaClO_4$ (0.50 g) was heated to reflux and cooled slowly to room temperature to give **5** in the form of single crystals suitable for an X-ray structural analysis. − IR (KBr): ν = 3263 cm^{-1}, 2964, 1576, 1464, 1145 (ClO_4 str), 1116 (ClO_4 str), 1088 (ClO_4 str), 1031, 1020, 822, 626. − ^{1}H NMR ([D$_6$]DMSO, room temp.; all signals paramagnetically broadened) δ = 1 (-CH_3), 20 (H^4), 43 (H^3), 100 (-CH_2-), 128 (-NH_2). − $C_{13}H_{25}Cl_2N_5NiO_8$ (508.99): calcd. C 30.68, H 4.95, N 13.76; found C 30.70, H 5.08, N 13.50.

*[(**1**)Ni(μ-Cl)Ni(**1**)](PF$_6$)$_3$* (**6**): To a solution of **2** (0.42 g, 1.00 mmol) in water (20 ml) was added a saturated aqueous solution of NH_4PF_6 (10 ml). The purple crystalline precipitate that formed was centrifuged, recrystallised from hot water, removed by filtration, washed with water, and air-dried. The resulting crystals were suitable for an X-ray structural analysis. Yield: 0.35 g (0.32 mmol, 64%). − IR (KBr): ν = 3374 cm^{-1}, 2967, 1603, 1579, 1469, 1397, 1084, 1020, 850 (PF_6), 559. − $C_{26}H_{50}ClF_{18}N_{10}Ni_2P_3$ (1090.52): calcd. C 28.64, H 4.62, N 12.84; found C 28.23, H 4.63, N 12.52.

*[(**1**)Ni(NCS)](PF$_6$)* (**7**): A solution of **2** (0.67 g, 1.68 mmol) in water (20 ml) was loaded onto a cation exchange column (Sephadex

Table 3. Crystallographic data for compounds **4**, **5**, **6**, **7** and **8**

	4	**5**	**6**	**7**	**8**
empirical formula	$C_{13}H_{27}I_2N_5NiO$	$C_{13}H_{25}Cl_2N_5NiO_8$	$C_{26}H_{50}ClF_{18}N_{10}Ni_2P_3$	$C_{14}H_{25}F_6N_6NiPS$	$C_{13}H_{25}F_6N_8NiP$
mol. mass	581.91	508.99	1090.54	513.14	497.09
crystal system	monoclinic	orthorhombic	tetragonal	monoclinic	monoclinic
space group (no.)	$P2_1/n$ (no. 14)	$Pna2_1$ (no. 33)	$I4_1cd$ (no. 110)	$P2_1/n$ (no. 14)	$P2_1/c$ (no. 14)
a [A]	9.936(2)	20.705(3)	21.312(3)	11.735(5)	10.703(1)
b [A]	18.804(5)	11.378(1)	21.312(3)	14.447(5)	11.059(1)
c [A]	10.757(3)	8.715(1)	19.010(4)	13.877(6)	17.130(1)
α [°]	90	90	90	90	90
β [°]	92.70(2)	90	90	113.65(3)	94.335(7)
γ [°]	90	90	90	90	90
Z	4	4	8	4	4
V [A^3]	2007.6(9)	2053.1(5)	8635(2)	2155(2)	2021.8(3)
ρ_{calcd} [g cm^{-3}]	1.925	1.647	1.678	1.582	1.633
diffractometer	Nicolet R3m/V	Enraf Nonius CAD4	Siemens P4	Nicolet R3m/V	E. Nonius MACH3
radiation	Mo-K_α	Mo-K_α	Mo-K_α	Mo-K_α	Mo-K_α (rotating anode)
monochromator	graphite	graphite	graphite	graphite	graphite
crystal size [mm^3]	0.60 × 0.40 × 0.40	0.36 × 0.20 × 0.12	0.70 × 0.40 × 0.40	0.45 × 0.30 × 0.25	0.40 × 0.20 × 0.20
T [°C]	293(2)	293(2)	200(2)	293(2)	293(2)
scan	ω	ω-2Θ	ω	ω	ω-Θ
2Θ range	4 ≤ 2Θ ≤ 54	5 ≤ 2Θ ≤ 53	4 ≤ 2Θ ≤ 48	4 ≤ 2Θ ≤ 54	5 ≤ 2Θ ≤ 48
measured reflections	5390	2219	7581	5761	3208
unique reflections	4382	2219	1967	4692	3164
observed reflections[a]	3246	1695	1360	1910	2095
μ(Mo-K_α) [mm^{-1}]	4.050	1.256	1.158	1.135	1.110
refined parameters	300	263	274	362	362
data/parameter ratio	14.6	8.4	7.2	13.0	8.7
*wR*2 (all data)[b]	0.0665	0.1460	0.1996	0.1250	0.1517
*R*1 (obs. data)[c]	0.0289	0.0508	0.0702	0.0518	0.0522
ρ_{fin}(max/min) [e A^{-3}]	0.771/−0.557	0.640/−0.358	1.514/−0.608	0.278/−0.514	0.837/−0.491
weighting scheme[d]	k = 0.0375/l = 0	k = 0.0757/l = 1.6931	k = 0.065/l = 54.317	k = 0.0536/l = 0	k = 0.0794/l = 3.1450

[a] With $F_o \geq 4\,\sigma(F)$; [b] $wR2 = (\{\Sigma[w(F_o^2 - F_c^2)^2]\}/\{\Sigma[w(F_o^2)^2]\})^{0.5}$; [c] $R1 = \Sigma||F_o| - |F_c||/\Sigma|F_o|$ for $F > 4\sigma(F)$; [d] $w = 1/[\sigma^2(F_o^2) + (k \cdot P)^2] + l \cdot P$ and $P = (F_o^2 + 2 \cdot F_c^2)/3$

SPC-25, ∅ 30 mm, length 190 mm), and the column eluted with water (200 ml). Gradient elution with an aqueous solution of NH_4SCN (0.1 M, 150 ml) removed a purple eluate which was concentrated to a volume of 20 ml. To this solution was added a saturated aqueous solution of NH_4PF_6 (10 ml). A single crystalline precipitate formed after several days. – IR (KBr): ν = 3274 cm^{-1}, 2979, 2091 (SCN), 1597, 1465, 1062, 1009, 850 (PF_6), 558. – $C_{14}H_{25}F_6N_6NiPS$ (513.13): calcd. C 32.77, H 4.91, N 16.38; found C 33.03, H 5.24, N 16.44.

*[(**1**)Ni(N$_3$)](PF$_6$)* (**8**): A solution of **2** (0.70 g, 1.75 mmol) in water (25 ml) was loaded onto a cation exchange column (Sephadex SPC-25, ∅ 30 mm, length 190 mm), and the column eluted with water (200 ml). Gradient elution with an aqueous solution of NaN_3 (0.1 M, 200 ml) removed a purple eluate which was taken to dryness. The remaining solid was taken up in methanol (50 ml), the suspension filtered to remove excess NaN_3, and the filtrate again taken to dryness. The residue was dissolved in water (10 ml), and the solution added to a concentrated aqueous solution of NH_4PF_6 (5 ml). The purple precipitate which had formed after several days was removed by filtration, washed quickly with a small amount of cold water, and air-dried. Single crystals suitable for an X-ray structural analysis were obtained by recrystallization from water. – IR (KBr): ν = 3256 cm^{-1}, 2962, 2060 (N_3), 1606, 1467, 1019, 834 (PF_6), 558. – $C_{13}H_{25}F_6N_8NiP$ (497.07): calcd. C 31.41, H 5.07, N 22.54; found C 30.94, H 4.88, N 20.52. Repeated recrystallizations gave samples which analysed consistently too low for N and, to a lesser extent, for C.

[1] H. M. Colquhoun, J. F. Stoddart, D. J. Williams, *Angew. Chem.* **1986**, *98,* 483–503; *Angew. Chem., Int. Ed. Engl.* **1986**, *25*, 487–507.
[2] J. E. Kickham, S. J. Loeb, S. L. Murphy, *Chemistry – A European Journal* **1997**, *3*, 1203–1213.
[3] A. Grohmann, F. Knoch, *Inorg. Chem.* **1996**, *35*, 7932–7934.
[4] E. Ahmed, C. Chatterjee, C. J. Cooksey, M. L. Tobe, G. Williams, M. Humanes, *J. Chem. Soc., Dalton Trans.* **1989**, 645–654.
[5] M. E. de Vries, R. M. La Crois, G. Roelfes, H. Kooijman, A. L. Spek, R. Hage, B. L. Feringa, *J. Chem. Soc., Chem. Commun.* **1997**, 1549–1550.
[6] A. J. Canty, N. J. Minchin, B. W. Skelton, A. H. White, *J. Chem. Soc., Dalton Trans.* **1986**, 2205–2210.
[7] D. H. Busch, *Chem. Rev.* **1993**, *93*, 847–860.
[8] D. H. Busch in *Proceedings of the First Hanford Separation Science Workshop*; Battelle Memorial Institute, Richland, WA, **1993**, p. II.9– II.14.
[9] C.- H. Lee, B. Garcia, T. C. Bruice, *J. Am. Chem. Soc.* **1990**, *112*, 6434–6435.
[10] O. Kahn, *Molecular Magnetism*; VCH, New York, **1993**, and references therein.
[11] A. E. Martell, R. D. Hancock, *Metal Complexes in Aqueous Solution*; Plenum Press, New York, **1996**, p. 39.
[12] A. McAuley, S. Subramanian, T. W. Whitcombe, *Can. J. Chem.* **1989**, *67*, 1650–1656.
[13] A. Bondi, *J. Phys. Chem.* **1964**, *68*, 441–451.
[14] S. Schmidt, L. Omnes, F. W. Heinemann, J. Kuhnigk, C. Krüger, A. Grohmann, *Z. Naturforsch.* **1998**, *53b*, *submitted*.
[15] J. L. Atwood, G. W. Orr, F. Hamada, R. L. Vincent, S. G. Bott, K. D. Robinson, *J. Am. Chem. Soc.* **1991**, *113*, 2760–2761.
[16] E. Kimura, T. Koike, H. Nada, Y. Iitaka, *Inorg. Chem.* **1988**, *27*, 1036–1040.
[17] G. Socrates, *Infrared Characteristic Group Frequencies;* 2nd edn.; Wiley, Chichester, **1994**, p. 220.
[18] T. C. Higgs, C. J. Carrano, *Inorg. Chem.* **1997**, *36*, 298–306.
[19] N. W. Alcock, K. P. Balakrishnan, P. Moore, H. A. A. Omar, *J. Chem. Soc., Dalton Trans.* **1987**, 545–550.
[20] M. A. Bennett, J. C. Jeffery, G. B. Robertson, *Inorg. Chem.* **1981**, *20*, 323–330.
[21] A recent search of the Cambridge Structural Database gave one example each of a fluoro- and bromo- bridged species:[21a] J. Emsley, M. Arif, P. A. Bates, M. B. Hursthouse, *J. Chem. Soc., Dalton Trans.* **1989**, 1273–1276;[21b] ref.[22].
[22] M. G. B. Drew, D. H. Templeton, A. Zalkin, *Inorg. Chem.* **1968**, *7*, 2618–2624.
[23] T. Kajiwara, T. Yamaguchi, H. Oshio, T. Ito, *Bull. Chem. Soc. Jpn.* **1994**, *67*, 2130–2135.
[24] M. Monfort, C. Bastos, C. Diaz, J. Ribas, X. Solans, *Inorg. Chim. Acta* **1994**, *218*, 185–188.
[25] R. Vicente, A. Escuer, J. Ribas, X. Solans, *J. Chem. Soc., Dalton Trans.* **1994**, 259–262.
[26] M. Taniguchi, A. Ouchi, *Bull. Chem. Soc. Jpn.* **1986**, *59*, 3277–3278.
[27] J. Ribas, M. Monfort, B. Kumar Ghosh, X. Solans, M. Font-Bardıa, *Polyhedron* **1996**, *15*, 1091–1095.
[28] S. Brooker, V. McKee, *J. Chem. Soc., Dalton Trans.* **1990**, 3183–3188.
[29] C. G. Pierpont, D. N. Hendrickson, D. M. Duggan, F. Wagner, E. K. Barefield, *Inorg. Chem.* **1975**, *14*, 604–610.
[30] M. K. Urtiaga, M. I. Arriortua, I. G. De Muro, R. Cortes, *Acta Crystallogr., Sect. C* **1995**, *51*, 62–65.
[31] Panmig Jian, Shuangxi Wang, Jishuan Suo, Liufang Wang, Qiangjin Wu, *Acta Crystallogr., Sect. C* **1995**, *51*, 1071–1073.
[32] P. Chaudhuri, M. Guttmann, D. Ventur, K. Wieghardt, B. Nuber, J. Weiss, *J. Chem. Soc., Chem. Commun.* **1985**, 1618–1620.
[33] F. Paap, W. L. Driessen, J. Reedijk, B. Kojic-Prodic, A. L. Spek, *Inorg. Chim. Acta* **1985**, *104*, 55–62.
[34] F. Wagner, M. T. Mocella, M. J. D′Aniello, Jr., A. H.-J. Wang, E. K. Barefield, *J. Am. Chem. Soc.* **1974**, *96*, 2625–2627.
[35] J. D. Atwood, *Inorganic and organometallic reaction mechanisms;* 2nd ed.; VCH, New York, NY, **1997**, p. 48.
[36] S. F. A. Kettle, *Physical Inorganic Chemistry, A Coordination Chemistry Approach*; Spektrum, Oxford, **1996**, p. 92.
[37] J. Ribas, M. Monfort, B. Kumar Ghosh, R. Cortes, X. Solans, M. Font-Bardıa, *Inorg. Chem.* **1996**, *35*, 864–868.
[38] G. A. McLachlan, G. D. Fallon, R. L. Martin, B. Moubaraki, K. S. Murray, L. Spiccia, *Inorg. Chem.* **1994**, *33*, 4663–4668.
[39] A. Escuer, R. Vicente, J. Ribas, M. S. El Fallah, X. Solans, M. Font-Bardıa, *Inorg. Chem.* **1993**, *32*, 3727–3732.
[40] M. Monfort, J. Ribas, X. Solans, *Inorg. Chem.* **1994**, *33*, 4271–4276.
[41] C. Butzlaff, A. X. Trautwein, H. Winkler in *Methods in Enzymology* (Eds.: J. F. Riordan, B. L. Valee), Academic Press, San Diego, **1993**, vol. 227; p. 412; ref.[10], p. 112.
[42] R. Vicente, A. Escuer, J. Ribas, M. S. El Fallah, X. Solans, M. Font-Bardıa, *Inorg. Chem.* **1995**, *34*, 1278–1281.
[43] A. Escuer, R. Vicente, J. Ribas, M. S. El Fallah, X. Solans, *Inorg. Chem.* **1993**, *32*, 1033–1035.
[44] P. Roman, C. Guzman-Miralles, A. Luque, J. I. Beitia, J. Cano, F. Lloret, M. Julve, S. Alvarez, *Inorg. Chem.* **1996**, *35*, 3741–3751.
[45] J. J. Borras-Almenar, E. Coronado, J. Curely, R. Georges, *Inorg. Chem.* **1995**, *34,* 2699–2704.
[46] B. Cabezon, A. Sastre, T. Torres, W. Schäfer, J. J. Borras-Almenar, E. Coronado, *J. Chem. Soc., Dalton Trans.* **1995**, 2305–2310.
[47] L. Ballester, E. Coronado, A. Gutierrez, A. Monge, M. F. Perpinan, E. Pinilla, T. Rico, *Inorg. Chem.* **1992**, *31,* 2053–2056.
[48] C. J. Gomez-Garcıa, E. Coronado, L. Ouahab, *Angew. Chem.* **1992**, *104,* 660–662; *Angew. Chem., Int. Ed. Engl.* **1992**, *31*, 649–651.
[49] E. Coronado, M. Drillon, A. Fuertes, D. Beltran, A. Mosset, J. Galy, *J. Am. Chem. Soc.* **1986**, *108*, 900–905.
[50] C. J. Ballhausen, *Introduction to Ligand Field Theory*; McGraw-Hill, New York, **1962**, p. 129.
[51] A. McAuley, S. Subramanian, T. W. Whitcombe, *J. Chem. Soc., Dalton Trans.* **1993**, 2209–2214.
[52] SHELXTL 5.03 for Siemens Crystallographic Research Systems, Copyright **1995** by Siemens Analytical X-Ray Instruments Inc., Madison, WI, USA.
[53] G. M. Sheldrick, SHELXS-86, Programme for Crystal Structure Solution, Universität Göttingen, **1986**.
[54] G. M. Sheldrick, SHELXL-93, Programme for Crystal Structure Refinement, Universität Göttingen, **1993**.

[97319]